Comparing Image-Based Respiratory Motion Correction Methods for Anatomical Roadmap Guided Cardiac Electrophysiology Procedures

YingLiang Ma[1], Andy P. King[1], Nicolas Gogin[2], Geert Gijsbers[3], C. Aldo Rinaldi[4], Jaswinder Gill[4], Reza Razavi[1], and Kawal S. Rhode[1]

[1] Division of Imaging Sciences, King's College London, SE1 7EH, UK
[2] Medisys Research Lab, Philips Healthcare, France
[3] Philips Healthcare, Netherlands
[4] Department of Cardiology, Guy's & St. Thomas' Hospitals NHS Foundation Trust, London, SE1 7EH, UK
y.ma@kcl.ac.uk

Abstract. X-ray fluoroscopically guided cardiac electrophysiological procedures are routinely carried out for diagnosis and treatment of cardiac arrhythmias. X-ray images have poor soft tissue contrast and, for this reason, overlay of static 3D roadmaps derived from pre-procedural volumetric data can be used to add anatomical information. However, the registration between the 3D roadmap and the 2D X-ray data can be compromised by patient respiratory motion. Three methods were evaluated to correct for respiratory motion using features in the X-ray image data. The first method is based on tracking either the diaphragm or the heart border using the image intensity in a region of interest. The second method detects the tracheal bifurcation using the generalized Hough transform and a 3D model derived from pre-operative image data. The third method is based on tracking the coronary sinus (CS) catheter. All three methods were applied to X-ray images from 18 patients undergoing radiofrequency ablation for the treatment of atrial fibrillation. The 2D target registration errors (TRE) at the pulmonary veins were calculated to validate the methods. A TRE of 1.6 mm ± 0.8 mm was achieved for the diaphragm tracking; 1.7 mm ± 0.9 mm for heart border tracking; 1.9 mm ± 1.0 mm for trachea tracking and 1.8 mm ± 0.9 mm for CS catheter tracking. We also present a comparison between our techniques with other published image-based motion correction strategies.

1 Introduction

Cardiac electrophysiological (EP) procedures are traditionally carried out under X-ray fluoroscopic guidance to diagnose and treat cardiac arrhythmias. However, X-ray images have poor soft tissue contrast and it is difficult to interpret the anatomical context directly from these images. To overcome the lack of soft tissue contrast, a three-dimensional (3D) roadmap can be generated from 3D high-resolution computed tomography (CT)/ magnetic resonance images (MRI), registered and overlaid in real-time with X-ray fluoroscopy images [1]. Currently, the 3D roadmap remains static and does not move with the patient's respiratory motion. In some cases, respiratory motion can cause a two-dimensional (2D) registration error of over 14 mm [2], which

D.N. Metaxas and L. Axel (Eds.): FIMH 2011, LNCS 6666, pp. 55–62, 2011.

is a significant compromise in the accuracy of guidance. A number of groups have addressed the issue of respiratory motion correction in the literature. Motion-compensated navigation for coronary interventions based on magnetic tracking was suggested in [3], but it required additional special hadware. Several image-based approaches have been developed that use only information from the X-ray fluoroscopic images themselves. Shechter et al. [4] constructed a model of cardiac and respiratory motion of the coronary arteries from biplane contrast-enhanced X-ray image sequences. The model was applied by tracking the motion of the diaphragm in subsequent (non-enhanced) X-ray images. However, forming the model from X-ray images under contrast injection means that it will be constructed from a limited amount of data. Furthermore, the diaphragm is not always in the X-ray field of view, particularly for obese patients. Brost et al. [5] developed an image-based respiratory motion correction method for EP procedures by tracking the 3D position of a lasso catheter from biplane X-ray images. Unlike tracking the diaphragm, this method directly tracks an instrument very close to the target region of the EP procedure. However, it also has some limitations. Firstly, the lasso catheter is particular for only a subset of EP procedures and it does not always remain stationary inside the heart. Secondly, the majority of X-ray systems are monoplane systems. Finally, the maximum frame rate of the lasso catheter tracking was only 3 frames per second and the tracking method required manual initialization.

The aim of our study was to develop and clinically evaluate respiratory motion compensation techniques for anatomical roadmapping for guiding cardiac EP interventions, particularly catheter radiofrequency ablation (RFA) for atrial fibrillation (AF), which is now one of the most common reasons for cardiac catheterization. The techniques needed to have accuracy within the clinical requirement of less than 5mm (determined by the typical size of the targeted structures, i.e. the PVs). They needed to be clinically robust and also have minimal interference with the routine clinical workflow. For the latter reason, we opted for approaches that used features present in the X-ray fluoroscopy image data, i.e. 2D image-based motion correction methods. Three approaches were implemented and clinically evaluated. The first method was based on tracking the diaphragm or the heart border, both of which are commonly observed in cardiac fluoroscopic images, even at very low radiation doses. This method tracks the image intensity within a manually defined rectangular region of interest (ROI) that lies across the diaphragm or heart border. The second approach that was used was to automatically track the tracheal bifurcation using the generalized Hough transform (GHT) for detection. The third method was to track the coronary sinus (CS) catheter from X-ray images using a catheter detection technique. We validate these three methods by computing the 2D target registration errors (TRE) at the pulmonary veins. In addition, we compare our methods with other published methods in the terms of speed, accuracy and robustness.

2 Method

2.1 Diaphragm or Heart Border Tracking

For the diaphragm or heart border tracking technique, a rectangular ROI was manually selected in which the motion of the diaphragm or heart border was visible

and no other radiographically dense features were present (see figure 1). One X-ray image was chosen as a reference. The diaphragm or heart border motion of subsequent X-ray images was determined by computing the 1D translation (along the long axis of the rectangle) that minimised the mean sum of squared differences between the intensities in the current image and the reference image within the ROI. A simple translational model similar to the one commonly employed in MRI image acquisition [6] was used to apply the 1D displacement of the diaphragm or heart border to the 3D heart roadmap. The 1D motion scaling factor for diaphragm was set to 0.6 (same as used in MRI) and the 1D motion scaling factor for heart border was set to 1 as heart was tracked directly. Finally, the 3D heart roadmap was translated along the head-to-foot vector of the patient by the 1D displacement.

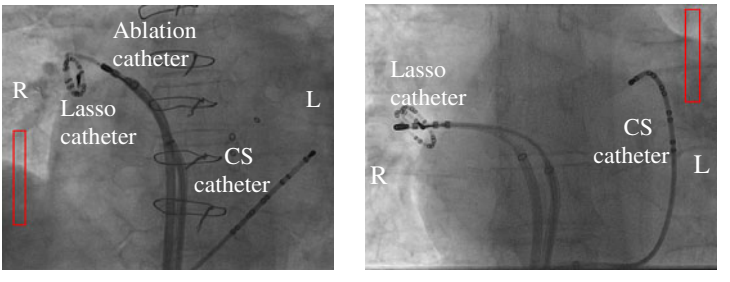

(a) diaphragm tracking (b) heart border tracking

Fig. 1. Tracking diaphragm (panel a) and tracking heartborder (panel b) in EP X-ray images. Red rectangle is the region of interest.

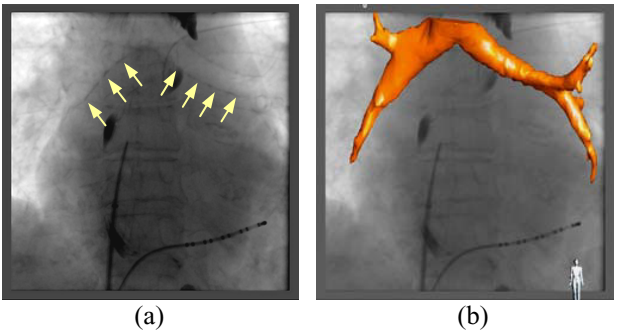

(a) (b)

Fig. 2. (a) An X-ray image showing the tracheal bifurcation. (b) A 3D model of the tracheal bifurcation derived from CT data is overlaid on to the X-ray fluoroscopic image.

2.2 Tracheal Bifurcation Detection

The tracheal bifurcation is located immediately above the LA and moves in a similar way to the LA during respiratory motion. It is clearly visible in cardiac X-ray fluoroscopic images (figure 2a). The Generalized Hough Transform (GHT) was used to detect the bifurcation in the X-ray images. A 3D model of the trachea (figure 2b) was derived from the pre-operative image data and then registered and projected onto the X-ray images to produce a 2D contour model. The contour model was used as a

template to match similar shapes in the X-ray images using the GHT. For tracking the tracheal bifurcation in X-ray fluoroscopic images, a Gaussian smoothing filter was first applied to the X-ray image followed by a Canny edge detector using the Sobel operator to find all edges. The edge map was then binarized using Otsu's algorithm [7] and the edges were iteratively thinned until they were one-pixel wide. Finally the contour model is used to search the optimal matched position in the binarized edge map using the GHT.

2.3 CS Catheter Detection

We developed a real time CS catheter tracking technique in [8]. This method first uses a fast multi-scale blob detection method to detect all possible electrode-like objects in the X-ray image. Based on prior knowledge of the CS catheter geometry, a cost function was designed to identify the CS catheter from all catheter-like objects. The reason for choosing the CS catheter instead of other catheters is that it is ubiquitously present during EP procedures. The CS catheter has several electrodes which are highly visible in normal dose and low dose X-ray images. Furthermore, the CS catheter remains in place throughout the procedure, its position is not routinely altered and it is normally not close to other catheters. Figure 3 gives an example of CS catheter detection.

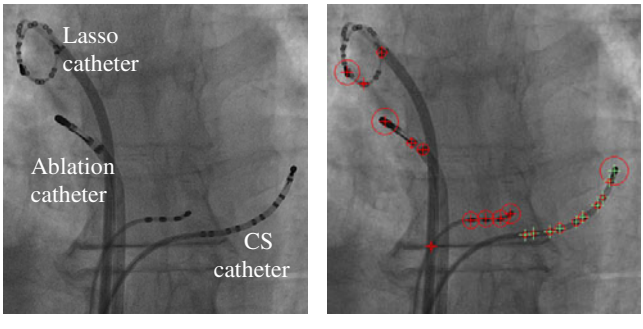

Fig. 3. An example result from the CS catheter detection method. Green crosses are the positions of CS catheter electrodes. Red crosses are the positions of other catheter electrodes. The size of the red circles represents the strength of the blobs.

3 Results

The tracking errors of the methods are first given. CS catheter tracking error was presented in [8] and we achieved 2D detection error of 0.39 mm ± 0.22 mm for all electrodes of the CS catheter. Then the validation of the motion correction methods is presented using the lasso catheter.

3.1 Diaphragm and Heart Border Tracking Errors

A clinical expert manually picked a center point along the border of the diaphragm or heart within the rectangular ROI. The error of tracking is defined as the 1D absolute

difference between the manually tracked point and the automatically tracked point along the long axis of the region of the interest. 1145 clinical X-ray fluoroscopic images were used to test the accuracy of tracking. There were a total of 25 different clinical fluoroscopy sequences which came from 18 clinical EP cases. 29% of the clinical X-ray images that were tested were low dose and contained high frequency noise. All X-ray images were 512×512 pixels in resolution. To estimate the ratio from pixel to mm R_{xray} in X-ray images, the X-ray DICOM file header information is used. Although the DICOM header gives the ratio R_{dicom} from pixel to mm, it is only correct when the magnification factor M of X-ray system is 1.0. The magnification factor M is computed using $M = D_{\det} / D_{pat}$, where $D_{\det}$ is the distance from X-ray source to the detector and D_{pat} is the distance from X-ray source to the patient. Finally, $R_{xray} = R_{dicom} / M$. The errors of diaphragm and heart border tracking in normal dose X-ray images were 1.2 ± 0.9 pixels (0.3 ± 0.2 mm). The errors in low dose X-ray images were 1.9 ± 1.3 pixels (0.5 ± 0.3 mm).

3.2 Tracheal Bifurcation Detection Errors

The tracheal bifurcation detection method was evaluated on the same dataset. However, only the X-ray sequences with the tracheal bifurcation within the field of view were selected. The total number of X-ray images used was 954 from 20 sequences which came from 18 clinical EP cases. 32% of the X-ray images were low dose and contained high frequency noise. The 3D models of the tracheal bifurcation were derived from pre-operative image data. There were 6 clinical cases using CT data, 4 cases using rotation X-ray angiography (RXA) and 8 cases using MRI. The tracheal bifurcation was automatically segmented from 3D high-resolution whole heart image data using a region growing algorithm followed by manual correction. To evaluate the detection errors, the bifurcation point was manually annotated on each X-ray frame by a clinical expert. This provided the ground-truth. The 3D trachea model was manually registered with a 2D X-ray image. In the subsequent frames, 2D translations were applied to the 2D trachea contour model. The detection errors were defined as the 2D distance between the manually defined bifurcation point and the bifurcation point in the trachea contour model. The model was positioned in 2D by the highest score from the GHT. Table 1 gives the errors of the trachea detection. All calculations were carried out on 512×512 resolution X-ray images.

Table 1. The 2D errors of the tracheal bifurcation detection. (Two figures are given for each modality: the 50% and 95% percentile errors. These represent the maximum detection errors of the lowest 50% and 95% of the tests respectively.).

	CT		MR		RXA	
	50%	95%	50%	95%	50%	95%
Normal dose image	1.9 pixels 0.5 mm	2.7 pixels 0.7 mm	7.7 pixels 2.1 mm	48.7 pixels 12.8 mm	2.0 pixels 0.5 mm	3.1 pixels 0.8 mm
Low dose image	5.8 pixels 1.5 mm	40.4 pixels 10.5 mm	44.5 pixels 11.7 mm	55.5 pixels 14.6 mm	N/A	N/A

3.3 Validation Using the Lasso Catheter

The intended application of the image-based tracking techniques was to update the position of a 3D roadmap. Therefore, the target registration error (TRE) was computed for the main validation of the approaches. Previous papers [2, 4] have reported motion error figures as a percentage of the total motion recovered. The percentage of motion recovered is calculated as

$$M_{rec} = 100\% * (TRE_{before} - TRE_{after}) / TRE_{before}$$

where TRE_{before} and TRE_{after} are the TREs before and after respiratory motion correction. A lasso catheter is often used in EP procedures. The lasso catheter is normally placed inside the PVs to be used as a mapping/measurement catheter. For the image sequences in which the lasso catheter was used for validation of accuracy, it remained stable in one of the PVs for all the X-ray frames evaluated (assessed by a clinical expert). For validation using the lasso catheter, 1D or 2D translational motion is applied to the 2D position of the lasso catheter tip electrode which acts as a surrogate for the position of the PVs since it is rigidly placed within these structures during the procedure. For the diaphragm and heart border tracking based motion correction strategies, the 1D translation along the long axis of the ROI was used. For the trachea tracking based approach, 2D translational motion was directly used. For the CS catheter based approach, filtered 2D translational motion was used. The TRE was computed as the distance error between this predicted position of the lasso catheter tip electrode and the actual position of the lasso catheter tip electrode in the X-ray data. The positions of the lasso catheter tip were manually annotated by a clinical expert. The TRE was calculated at the PVs on 418 fluoro images (8 patients). All X-ray images are normal dose which is suitable for the trachea-based motion compensation approach. The pre-operative image was either CT or RXA data. Table 2 gives the comparison of TREs among all motion correction strategies.

Table 2. TRE before and after motion correction using lasso catheter validation

TRE (mm)	Diaphragm	Heart border	Trachea	CS catheter
Before	4.7 ± 1.7	4.7 ± 1.7	4.7 ± 1.7	4.7 ± 1.7
After	1.6 ± 0.8	1.7 ± 0.9	1.9 ± 1.0	1.8 ± 0.9
Motion Recovered	45%~75%	41%~74%	39%~71%	37%~72%

4 Conclusion and Discussions

Three image-based motion correction approaches have been developed and evaluated. Image-based approaches do not require any fiducial markers, additional contrast agent or special hardware and do not interfere with the clinical work-flow. Each approach has its advantages and disadvantages. Diaphragm tracking is fast and free of cardiac cycle motion. Heart border tracking is also fast but can be influenced by cardiac cycle

motion. However, considering the case of an obese patient, the diaphragm is not often in the field of view so heart border tracking can be used instead. Furthermore, diaphragm tracking requires a motion correction factor (0.6) which may not be valid for all patients. Both methods require manually defined ROIs which are free of other features such as guide wires or catheters. The ROI may have to be changed often due to C-arm rotation, changing contrast and features moving into the region of interest. However, from the experience of 18 clinical EP cases, tracking the heart border is easier than tracking the diaphragm as the heart border shadow often has better contrast than the shadow of the diaphragm and it is always in the field of view. In 2 cases, when the left heart border was tracked and the patient heart was aligned to the iso-center of the X-ray system, the ROI did not have to be changed even if the C-arm was rotated through the normal clinical range. Both methods are computationally efficient and simple to implement. Furthermore, as both methods track soft tissue, they can be used at anytime during EP procedures.

Tracking the trachea gives only respiratory motion and the trachea is very close to the primary target of left atrium of the procedures. However, it becomes less robust and accurate when it is used for low dose X-ray images. This is because low dose X-ray images have fewer strong edges for the tracheal bifurcation and this causes the GHT method to detect the wrong object. The trachea detection method requires a 3D model to generate the 2D GHT contour model. In this study, it was found that the pre-operative 3D MRI image data was least suitable for generating the 3D tracheal model. This was caused by the low contrast of the tracheal bifurcation in the MR images and the region growing method yielded a noisy and truncated model of the trachea. Truncated bronchi generate less edge information for the GHT contour model and the GHT becomes less robust. As a conclusion, the trachea detection based motion correction approach should be used in normal dose X-ray fluoroscopic images with a pre-operative 3D image data set acquired using CT or RXA. The 2D translational motion of the tracheal bifurcation can be directly applied to the 3D roadmap to correct respiratory motion.

As a fully automatic method, real-time CS catheter detection in X-ray fluoroscopy images was developed and it is accurate and robust even in low dose fluoroscopy images as CS catheter electrodes remain highly visible. A sub-millimeter accuracy of CS catheter detection method was achieved. Updating the 3D roadmap by the filtered 2D motion of the CS catheter can significantly improve the accuracy of fluoroscopy overlays for cardiac EP procedures. The CS catheter detection method has several advantages. First, it is real-time so that as well as being used to detect respiratory motion it could potentially also be applied to the detection of the much faster cardiac cycle motion. Secondly, it does not require any user interaction and can detect the CS catheter position without defining a ROI in the X-ray image. Similar to the diaphragm and heart border tracking based approaches, the CS catheter detection based motion correction does not restrict which kind of pre-operative 3D image data can be used. However, the presence of cardiac cycle motion in the CS catheter is a potential disadvantage for respiratory motion correction. Table 3 summarizes the comparison among the methods as well as the lasso catheter tracking based motion correction method [5], King et al.'s patient-specific motion correction method [2] and Shechter's prospective motion correction method [4].

Table 3. Comparison among respiratory motion correction methods. (unit of tracking speed is frames per second).

	Tracking error (mm)	Success rate	With cardiac motion	Tracking Speed	Motion Recovered (average)	X-ray Image Dose
Diaphragm	0.4 ± 0.3	100%	No	>30	65%	Low/Normal
Heart border	0.4 ± 0.3	100%	Yes	>30	63%	Low/Normal
Tracheal bifurcation	0.8 ± 0.2	96.7% *	No	3	61%	Normal
CS catheter	0.4 ± 0.2	99.3%	Yes	21	60%	Low/Normal
Lasso catheter	0.6 ± 0.3	N/A	Yes	3	N/A	N/A
King *et al.* Method	N/A	100%	No	>30	66%	Low/Normal
Shechter's Method	N/A	N/A	Yes	N/A	63%	Normal

A successful detection is defined as the detection error is within 5 mm, which is the radius of the pulmonary veins.
*Please note that the success rate of trachea detection excludes tests carried out on the low dose X-ray images and the clinical cases using MR pre-operative image data.

References

1. Rhode, K.S., Hill, D.L.G., Edwards, P.J., Hipwell, J., Rueckert, D., Sanchez-Ortiz, G., Hegde, S., Rahunathan, V., Razavi, R.: Registration and Tracking to Integrate X-ray and MR Images in an XMR facility. IEEE Transactions on Medical Imaging 24(11), 810–815 (2003)
2. King, A.P., Boubertakh, R., Rhode, K.S., Ma, Y.L., Chinchapatnam, P., Gao, G., Tangcharoen, T., Ginks, M., Cooklin, M., Gill, J.S., Hawkes, D.J., Razavi, R.S., Schaeffter, T.: A Subject-specific Technique For Respiratory Motion Correction in Image-guided Cardiac Catheterisation Procedures. Med. Image. Anal. 13(3), 419–431 (2009)
3. Timinger, H., Krueger, S., Dietmayer, K., Borgert, J.: Motion Compensated Coronary Interventional Navigation by Means of Diaphram Tracking and Elastic Motion Models. Phys. Med. Biol. 50(3), 491–503 (2005)
4. Shechter, G., Shechter, B., Resar, J.R., Beyar, R.: Prospective Motion Correction of X-ray Images for Coronary Interventions. IEEE Transactions on Medical Imaging 24(4), 441–450 (2005)
5. Brost, A., Liao, R., Hornegger, J., Strobel, N.: 3-D Respiratory Motion Compensation during EP Procedures by Image-based 3-D Lasso Catheter Model Generation and Tracking. In: Yang, G.-Z., Hawkes, D., Rueckert, D., Noble, A., Taylor, C. (eds.) MICCAI 2009. LNCS, vol. 5761, pp. 394–401. Springer, Heidelberg (2009)
6. Wang, Y., Riederer, S.J., Ehman, R.L.: Respiratory Motion of the Heart: Kinematics and the Implications for the Spatial Resolution in Coronary Imaging. Magnetic Resonance in Medicine 33(5), 713–719 (1995)
7. Otsu, N.: A Threshold Selection Method from Gray-level Histograms. IEEE Transactions on Systems, Man and Cybernetics 9(1), 62–66 (1979)
8. Ma, Y., King, A.P., Gogin, N., Rinaldi, C.A., Gill, J., Razavi, R., Rhode, K.S.: Real-Time Respiratory Motion Correction for Cardiac Electrophysiology Procedures Using Image-Based Coronary Sinus Catheter Tracking. In: Jiang, T., Navab, N., Pluim, J.P.W., Viergever, M.A. (eds.) MICCAI 2010. LNCS, vol. 6361, pp. 391–399. Springer, Heidelberg (2010)